Colloids and Surfaces B: Biointerfaces 223 (2023) 113156

Contents lists available at ScienceDirect

Colloids and Surfaces B: Biointerfaces

journal homepage: www.elsevier.com/locate/colsurfb

Eggshell membrane-incorporated cell friendly tough hydrogels with ultra-adhesive property

Yonghyun Gwon [a,b,c], Sunho Park [a,b], Woochan Kim [a,b,c], Hyoseong Kim [a,b,c], Jangho Kim [a,b,c,*]

[a] Department of Convergence Biosystems Engineering, Chonnam National University, Gwangju 61186, the Republic of Korea
[b] Department of Rural and Biosystems Engineering, Chonnam National University, Gwangju 61186, the Republic of Korea
[c] Interdisciplinary Program in IT-Bio Convergence System, Chonnam National University, Gwangju 61186, the Republic of Korea

ARTICLE INFO

Keywords:
Eggshell membrane
Adhesive hydrogel
Tough hydrogel
Cell friendly

ABSTRACT

Adhesive and tough hydrogels have received increased attention for their potential biomedical applications. However, traditional hydrogels have limited utility in tissue engineering because they tend to exhibit low biocompatibility, low adhesiveness, and poor mechanical properties. Herein, the use of the eggshell membrane (ESM) for developing tough, cell-friendly, and ultra-adhesive hydrogels is described. The ESM enhances the performance of the hydrogel network in three ways. First, its covalent cross-linking with the polyacrylamide and alginate chains strengthens the hydrogel network. Second, it provides functional groups, such as amine and carboxyl moieties, which are well known for enhancing the surface adhesion of biomaterials, thereby increasing the adhesiveness of the hydrogel. Third, it is a bioactive agent and improves cell adhesion and proliferation on the constructed scaffold. In conclusion, this study proposes the unique design of ESM-incorporated hydrogels with high toughness, cell-friendly, and ultra-adhesive properties for various biomedical engineering applications.

1. Introduction

Hydrogels are cross-linked polymer networks with a water content of more than 70 %. These biomaterials are emerging as promising soft scaffolds for tissue engineering applications owing to their similarities to living systems, such as their high water content, flexibility, softness, and permeability. In particular, because hydrogels have a similar structure and stiffness to soft tissues in the body, such as the skin, cartilages, muscles, and tendons, they are especially useful for the regeneration of such types of tissue [1,2]. However, hydrogels still have limited application in tissue engineering owing to their brittleness (caused by their high water content) and poor mechanical properties [3]. In the past decades, various attempts have been made to improve the mechanical properties of hydrogels with approaches such as ionic cross-linking, double cross-linking, and nanocomposite cross-linking of the polymer network [3–5]. Although some of these approaches have significantly improved the mechanical properties of tough hydrogels, the low adhesiveness of the constructs and the poor cell activity thereon remain major limitations to their wide application in tissue engineering [5,6]. Recently, a group of researchers have developed a tough hydrogel, based on an interpenetrating network of alginate and polyacrylamide chains, which displays remarkable mechanical properties [7]. This hydrogel has the mechanical strength and ability to stretch over 20 times its original length. Moreover, its combination of the naturally derived polymer alginate and polyacrylamide means that it has low cytotoxicity and thus good potential for use in biomedical applications [7]. However, despite the remarkable mechanical properties of this hydrogel, its application as a scaffold for tissue regeneration is still questionable owing to its low tissue adhesiveness, and its acrylamide monomers cast doubt on its biocompatibility and toxicity. Therefore, the development of an advanced hydrogel with exceptional toughness, biocompatibility, and bioactivity is still required.

The eggshell membrane (ESM), which separates the mineralized eggshell from the egg white, has a composition similar to that of the extracellular matrix [8]. Having long been treated as a waste product, its use in the field of tissue engineering has only recently begun to be valued. In its natural state, the ESM has the following advantages: (i) it is low in cost and can be easily obtained (even for free) from industrial and household wastes; (ii) it is a biocompatible and environmentally friendly material; (iii) it can combine stably with and allow the attachment of a wide range of biomaterials owing to its high surface area, excellent chemical stability, and high density of functional groups such as amines, amides, and carboxylic acids [8–10]; and (iv) it can be readily modified through carbonization and dissolution processes, allowing its

* Corresponding author at: Department of Convergence Biosystems Engineering, Chonnam National University, Gwangju 61186, the Republic of Korea.
E-mail address: rain2000@jnu.ac.kr (J. Kim).

https://doi.org/10.1016/j.colsurfb.2023.113156
Received 29 July 2022; Received in revised form 15 January 2023; Accepted 17 January 2023
Available online 18 January 2023

application in a variety of fields with the use of various engineering techniques [11]. Furthermore, 80–85 % of the ESM matrix is organic in nature, with the remaining 15–20 % being inorganic. The organic matrix consists of collagens (types I, V, and X), which are the major constituents of connective tissue (e.g., skin, tendon, and bone) and cartilage; osteopontin, which is a component of bone; and fibronectin, which promotes cell adhesion, migration, and differentiation during wound healing. Given these advantages and the strength of its components, the ESM has received more attention as a potential tissue engineering biomaterial in recent years [12,13]. Our research group has also been engineering and developing the ESM as a bioactive agent, and we have published several studies on its regulation of cellular behavior and functions for tissue regeneration [14,15]. Specifically, we found that the raw ESM could regulate the morphology, attachment, and proliferation of stem cells, and that soluble ESMs significantly promoted the osteogenic differentiation of osteoblasts and bone tissue regeneration [14,15].

On the basis of these findings, this study was carried out to develop an ESM-incorporated hydrogel that is tough, cell friendly, extremely stretchable, highly adhesive, and biocompatible for tissue engineering applications. It was expected that the mechanical properties (i.e., stretch and adhesive abilities) and biocompatibility (i.e., allowance for cell attachment and viability) of the hydrogel would be enhanced through the intrinsic properties of the ESM. Hydrogels were fabricated by mixing three types of cross-linked polymers (ionically cross-linked alginate chains, covalently cross-linked polyacrylamide chains, and covalently cross-linked alginate–ESM and polyacrylamide–ESM chains) to form a double-network structure. The resultant ESM-incorporated hydrogel was extremely tough and stretchable and exhibited an enhanced ability to adhere to various types of surfaces, including skin, glass, polypropylene, wood, steel, and titanium. Moreover, it showed improvement in the adhesion of mesenchymal stem cells, osteoblasts, and fibroblasts and in maintaining their viability. To the best of our knowledge, this is the first attempt in the use of the ESM for developing tough hydrogels.

2. Experimental section

2.1. Preparation of the ESM solution

To fabricate the ESM solution, the raw ESM was peeled off from the eggshell by hand. The separated ESM was then washed several times with distilled water, dried, and finally ground in a blender for 5 min. Thereafter, the ESM powder was dissolved in a solution containing 3-mercaptopropionic acid (Sigma-Aldrich, USA), acetic acid (Daejung Chemicals & Metals, Republic of Korea), and deionized water, with magnetic stirring at 1500 rpm, for 3 days on a 120 °C hotplate. The low-pH ESM solution was adjusted to a pH of 5 using sodium hydroxide (Sigma-Aldrich). Then, the neutralized sample was washed three times with methanol (Daejung Chemicals & Metals) and distilled water and dried in a vacuum oven at 70 °C for 2 h. Finally, the dried ESM powder was dissolved in 10 % acetic acid using a magnetic stirrer.

2.2. Design and fabrication of the ESM-incorporated hydrogel

Alginate–polyacrylamide hybrid gels were prepared using a previously described method [8]. In brief, alginate (Protanal LF 20/40, Sigma-Aldrich, USA) and acrylamide (Invitrogen, USA) were dissolved in water in a 1:6 ratio to obtain a final polymer concentration of 14 % in the gel. This solution was rapidly mixed with *N*, *N*′-methylenebisacrylamide (Invitrogen) as the acrylamide cross-linker, a calcium sulfate slurry (Sigma-Aldrich) as the alginate cross-linker, *N*, *N*,*N*′,*N*′-tetramethylethylenediamine (Invitrogen) as the acrylamide cross-linking accelerator, and ammonium persulfate (Sigma-Aldrich) as the acrylamide cross-linking photoinitiator. For all the experiments, the gels were prepared with four different acrylamide cross-linking densities: 0.06 wt% *N*,*N*′-methylenebisacrylamide relative to acrylamide, referred to as “optimal”; and 0.03 wt%, referred to as “low.” The optimal cross-linking density was used in all other interpenetrating polymer networks. Finally, 0.1 %, 0.5 %, or 1 % ESM solution (volume ratios of ESM to ESM + acrylamide) was added to the polymer solution and cross-linking was allowed to take place overnight before the hydrogels were removed from the mold. Polyacrylamide and alginate gels with no ESM incorporated were also prepared as controls, using the same weight percentage of polymer as in the hybrid gels. Before testing, the gels were washed for 30 h in serum-free Dulbecco’s modified Eagle’s medium (DMEM; Cellgro, USA).

2.3. Characterization of the ESM-incorporated Hydrogel

High-resolution FE-SEM images of the hydrogel surface were acquired using a JSM-7500F microscope (JEOL Ltd., Japan) at a magnification of × 5000 with an acceleration voltage of 15 kV. FTIR was performed using a Spectrum 400 system (PerkinElmer, USA) to confirm the chemical bond structures of the ESM-incorporated hydrogels. Spectra from the XPS analysis were recorded using a monochromatic Al Kα source (1486.67 eV) with a spot size of 200 μm and an electron take-off angle of 90°. The typical base pressure was below 2×10^{-9} mbar. The spectra were recorded in the range of 0–1350.0 eV with a pass energy value of 200 eV, step size of 1.0 eV, and dwell time of 10.0 ms.

2.4. Adhesion test

Adhesion test was performed to measure the adhesive strength of the ESM-incorporated hydrogels. The fabricated hydrogels were attached to the surface of various surfaces with a bonding area of 25 mm × 25 mm. The substrates chosen for investigation were glass, steel, polypropylene, rubber, wood, porcine skin, dECM dermis, SI wafer, and titanium, representing hydrophilic, hydrophobic, and metal materials. Porcine skin was chosen for mimicking adhesion to human tissue. The adhesion test was conducted immediately once the hydrogel was attached onto the substrate surface, which did not require a curing time. Normal adhesion was tested for resistance to peeling by attaching the hydrogel and porcine skin in parallel and shear adhesion was tested by attaching the hydrogel and porcine skin perpendicular to the peeling resistance.

2.5. Mechanical property test

The tensile and compression tests were performed using a universal test machine (Series 5567, Instron, USA). For tensile testing, specimens of 25 mm width and 3 mm thickness were used. For compression testing, hydrogels with a cylindrical shape (10 mm height and 5 mm diameter) were used. The fracture energy of each hydrogel was determined using the classical single-edge notched test on the same machine (Instron 5567). The strain-stress curve recorded during tests and the tensile stress, strain, and elastic modulus were calculated. In detail, young’s modulus is calculated following formula: young’s modulus=stress/strain.

2.6. Immunofluorescence assay

Adherent cells on the hydrogel were fixed with a 4 % paraformaldehyde solution (Biosesang, Korea) for 15 min and then permeabilized with 0.2 % Triton X-100 (Biosesang). The fixed cells were then blocked with 3 % normal goat serum (Abcam, USA) in phosphate-buffered saline (PBS; Biosesang). After a wash with PBS, the scaffolds were stained with 4′,6-diamidino-2-phenylindole (Millipore, USA) for 3 min. Images of the stained cells were obtained using a fluorescence microscope.

2.7. Cell attachment and proliferation assays

Osteoblast-like MG-63 cells, NIH-3T3 fibroblasts, and adipose-derived mesenchymal stem cells (1×10^4 cells/sample) were seeded

onto the various hydrogels. Before seeding, the prepared hydrogels were first purified in PBS and sterilized with 75 % ethanol for 24 h. The hydrogels were then immersed in DMEM and swelled to an equilibrium state. The PBS washing and ethanol disinfection procedures slightly swelled the hydrogels but did not affect their physical and biological properties. Then, the samples were then cultured in DMEM containing 10 % fetal bovine serum and 1 % antibiotics (Cellgro) for 6 h, 3 days, and 5 days at 37 °C in a humidified atmosphere containing 5 % CO2. Quantitative analysis of cell growth on the hydrogels was performed using the WST-1 assay with the Premix WST-1 Cell Proliferation Assay System (Takara Bio Inc., Japan). Prior to performing the cell proliferation assay, the hydrogels were washed with PBS to remove any non-adherent cells and thereby confirm cell attachment to the scaffolds.

2.8. Statistical analysis

All quantitative data are presented as the mean ± standard deviation. The results from the cell adhesion, viability experiments were statistically analyzed using the unpaired Student *t*-test. One-way analysis of variance was used to compare three or more conditions. Differences with a *P*-value of less than 0.05 were considered statistically significant.

3. Results and discussion

3.1. Design strategy for fabrication of the ESM-incorporated hydrogels

Inspired by the chemical stability and biocompatibility of the ESM, extremely stretchable and ultra-adhesive hydrogels were fabricated using four cross-linking steps. In the first step to generate the alginate hydrogel network, a calcium sulfate slurry ($CaSO_4{\cdot}2H_2O$) provides the divalent Ca^{2+} cations that act as ionic cross-linkers between the alginate chains (Fig. 1a). In the second step to generate the polyacrylamide hydrogel network, *N*,*N*′-methylenebisacrylamide is used to covalently cross-link the polyacrylamide chains, with ammonium persulfate applied as the photoinitiator for the process (Fig. 1a). In the third step to generate the alginate–polyacrylamide hybrid gel network, the polymer networks generated in the first two steps were mixed, whereupon they formed covalent cross-links with each other via the amine groups on the polyacrylamide chains and the carboxyl groups on the alginate chains. Finally, in the last step, dissolved ESM was added to the hybrid gel network and formed covalent cross-links in between the two types of polymer chains. That is, this final step may be the key for the fabrication of extremely stretchable, ultra-adhesive, and tough hydrogels. The strong bonds formed within the hydrogel network also improved its chemical stability.

As mentioned above, the ESM has excellent chemical stability and a high density of functional groups, such as amines, amides, and carboxylic acids. The amine and carboxyl groups on the ESM particles form covalent cross-links with the carboxyl groups on the alginate chains and the amine groups on the polyacrylamide chains, respectively (Fig. 1a). Fig. 1b shows field-emission scanning electron microscopy (FE-SEM) images of hydrogels with various concentrations of ESM incorporated (i.e., 0 %, 0.1 %, 0.5 %, and 1 %), indicating the highly interconnected macropores in the microstructures. Interestingly, the pore sizes of the hydrogel appeared smaller with increasing ESM concentration, which was due to the increased number of ESM particles binding to the polyacrylamide and alginate chains. The functional groups of the ESM-incorporated hydrogels were investigated by FT-IR spectroscopy (Fig. S2). The characteristic absorption bands related to ESM (i.e., C-H at 1380 cm^{-1}, C═C at 1480 cm^{-1}, N-H at 1620 cm^{-1}) were detected in all ESM-incorporated hydrogels groups, showing that functional groups were well maintained. The surface chemical composition of the ESM-incorporated hydrogels was analyzed by XPS. As shown in Fig. 1d, all XPS spectra had three separated peaks corresponding to O1s (285 eV), N1s (400 eV), and C1s (532 eV). A distinct N1s peak at 400 eV in the ESM-incorporated hydrogels spectrum indicated that the ESM components had been successfully penetrate hydrogel network. The surface atomic compositions of the 0.1 % ESM-hydrogels were calculated to be 74.83 %, 7.78 %, and 13.01 %, and those of the 0.5 % and 1 % ESM-hydrogels were calculated to be 69.81 %, 13.17 %, and 17.02 % for C1s, N1s, and O1s, respectively.

3.2. Adhesiveness of the ESM-incorporated hydrogels

The fabricated ESM-incorporated hydrogel had high adhesiveness to biological tissue, which is a key factor for biomedical applications. In particular, the construct adhered very well to human skin and left no sticky residue when peeled off (Fig. 2**a**). Interestingly, the fabricated hydrogel could adhere directly to both hydrophilic and hydrophobic surfaces, such as glass, steel, polypropylene, rubber, and wood (Fig. 2b). Additionally, it facilitated the adhesion of porcine skin, decellularized extracellular matrix (dECM) dermis, silicon wafer, and titanium to glass. To optimize the adhesiveness of the biomaterial, the adhesive strengths of the hydrogels (prepared with different ESM concentrations) to representative surfaces were quantified using the tensile adhesion test. As shown in Fig. 2d, the adhesive strength initially increased with increasing ESM concentration but then decreased when the concentration exceeded 0.5 %. Nonetheless, the hydrogels maintained a high degree of adhesion (> 20 kPa) to all tested surfaces, regardless of the amount of ESM incorporated, with the 0.5 % ESM-incorporated hydrogel exhibiting the best adhesive strength in the order of glass (45.8 kPa) > steel (41.5 kPa) > wood (41.3 kPa) > polypropylene (40.9 kPa) > rubber (37.1 kPa) > dECM dermis (29.7 kPa). To further investigate the adhesiveness of the fabricated hydrogels, their normal adhesion and shear adhesion to porcine skin and dECM dermis were compared. Similar to the previous results, the 0.5 % ESM-incorporated hydrogel showed the highest adhesive strength for both porcine skin and dECM dermis, with the normal and shear adhesive strengths to porcine skin being 31.8 and 28.4 kPa, respectively (Fig. 2e, f). These adhesive strength results are superior to those recently reported for other adhesive and tough hydrogels [16–18].

The high adhesiveness of the ESM-incorporated hydrogel is likely due to the functional groups of the ESM (i.e., the highly enriched amine and carboxyl groups), which can enhance the interactions between the hydrogel and various surfaces, as has been previously demonstrated [17, 19]. In the XPS analysis according to the concentration of ESM (0 %, 0.1 %, 0.5 % and 1 %), we observed the increase in functional groups, especially carboxyl (-COOH) and amino groups ($-NH_2$), on the hydrogel surface as the concentration of ESM increased (Figs. 1e and S1). The results showed higher amine ($-NH_2$) and carboxyl group (-COOH) peaks with increased ESM concentrations, corresponding to the enhancement in adhesive strength with increasing ESM particles incorporated in the hydrogel (Fig. 2d). Also, the results showed higher amine ($-NH_2$) and carboxyl group (-COOH) peaks with increased ESM concentrations. These results proved that both the amine and carboxyl groups of ESM contributed to the improved adhesiveness of the hydrogel [20-22].

3.3. Mechanical properties of the ESM-incorporated hydrogels

The fabricated hydrogel was resilient and sufficiently tough and could be stretched to 20 times its initial length (Fig. 3a). Furthermore, its areal strain exceeded 1600 % (Fig. 3b), rendering it suitable for complex deformations. For example, a fabricated hydrogel with an area of only 25 cm^2 was able to cover a cylinder of 8 cm diameter and 22 cm height (Fig. 3c). These results showed that the ESM-incorporated hydrogel was highly stable under various deformation conditions and could therefore be applied to different stress states. Uniaxial tensile tests were performed to confirm the mechanical properties of the hydrogels. Fig. 3d shows the typical tensile stress–strain curves of the hydrogels according to the different ESM concentrations. As expected, the stress–strain curves formed at high values as the ESM concentration was increased because

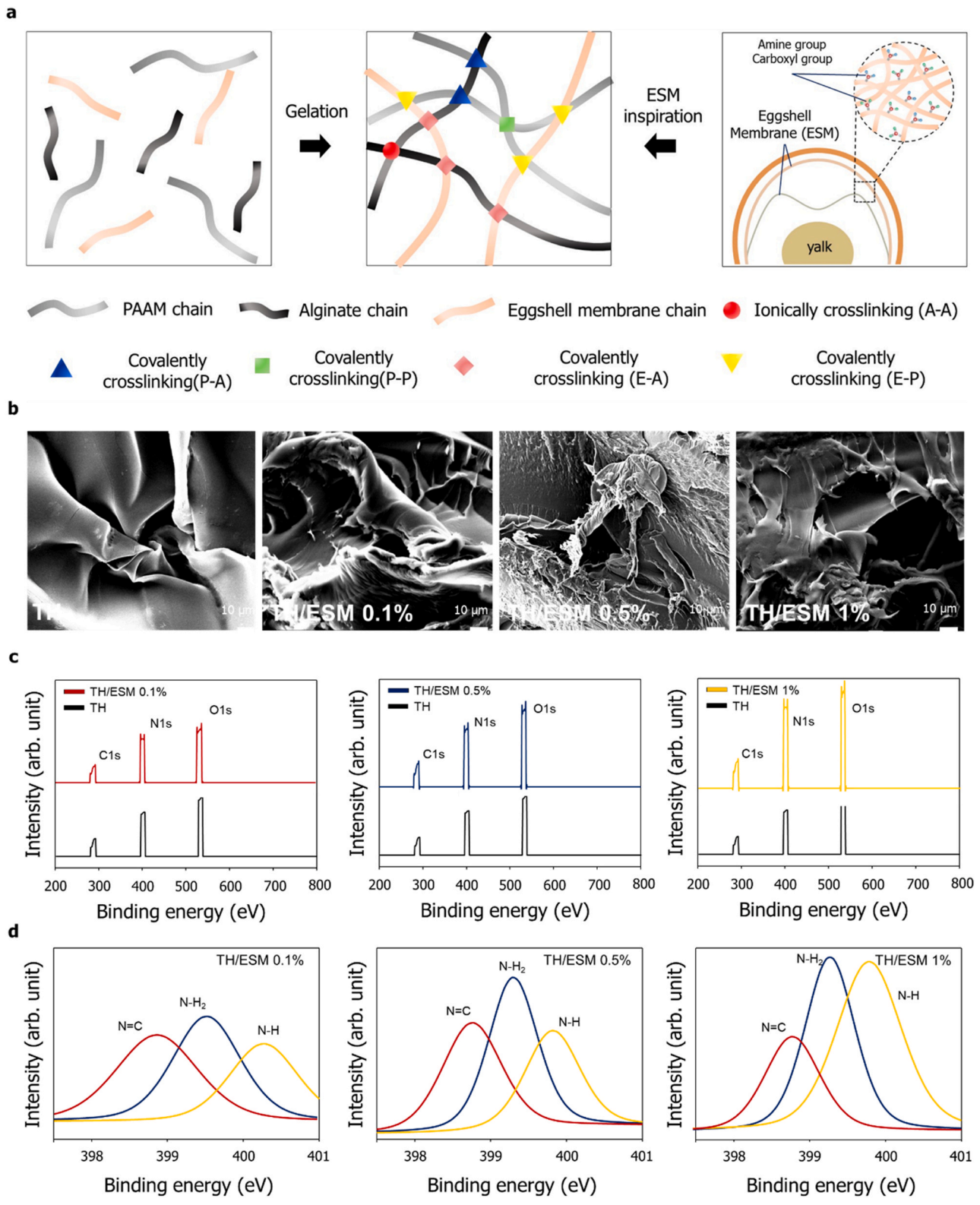

Fig. 1. Design strategy for the fabrication of bio-inspired eggshell membrane-incorporated hydrogels with high toughness and cell-friendly and ultra-adhesive properties. (a) In the alginate hydrogel network, the divalent cations Ca^{2+} act to cross-link the alginate chains ionically. In the polyacrylamide hydrogel network, polyacrylamide chains cross-link covalently with the aid of *N*,*N*′-methylenebisacrylamide. In the alginate–polyacrylamide hybrid gel network, the two types of polymer chains are intertwined and joined by covalent cross-links between the amine groups on the polyacrylamide chains and the carboxyl groups on the alginate chains. In the ESM-alginate and ESM-polyacrylamide hybrid network, ESMs are covalently cross-linked with the two polymer chains between the amine groups on the polyacrylamide chains and the carboxyl groups on the alginate chains. (b) FE-SEM images of hydrogels with various concentrations of ESM incorporated (0 %, 0.1 %, 0.5 %, and 1 %). (c,d) XPS spectra of hydrogels with various concentrations of ESM incorporated (0 %, 0,1 %, 0.5 %, and 1 % in order from above). E and ESM, eggshell membrane; P and PAAM, polyacrylamide; A, alginate; TH, tough hydrogel.

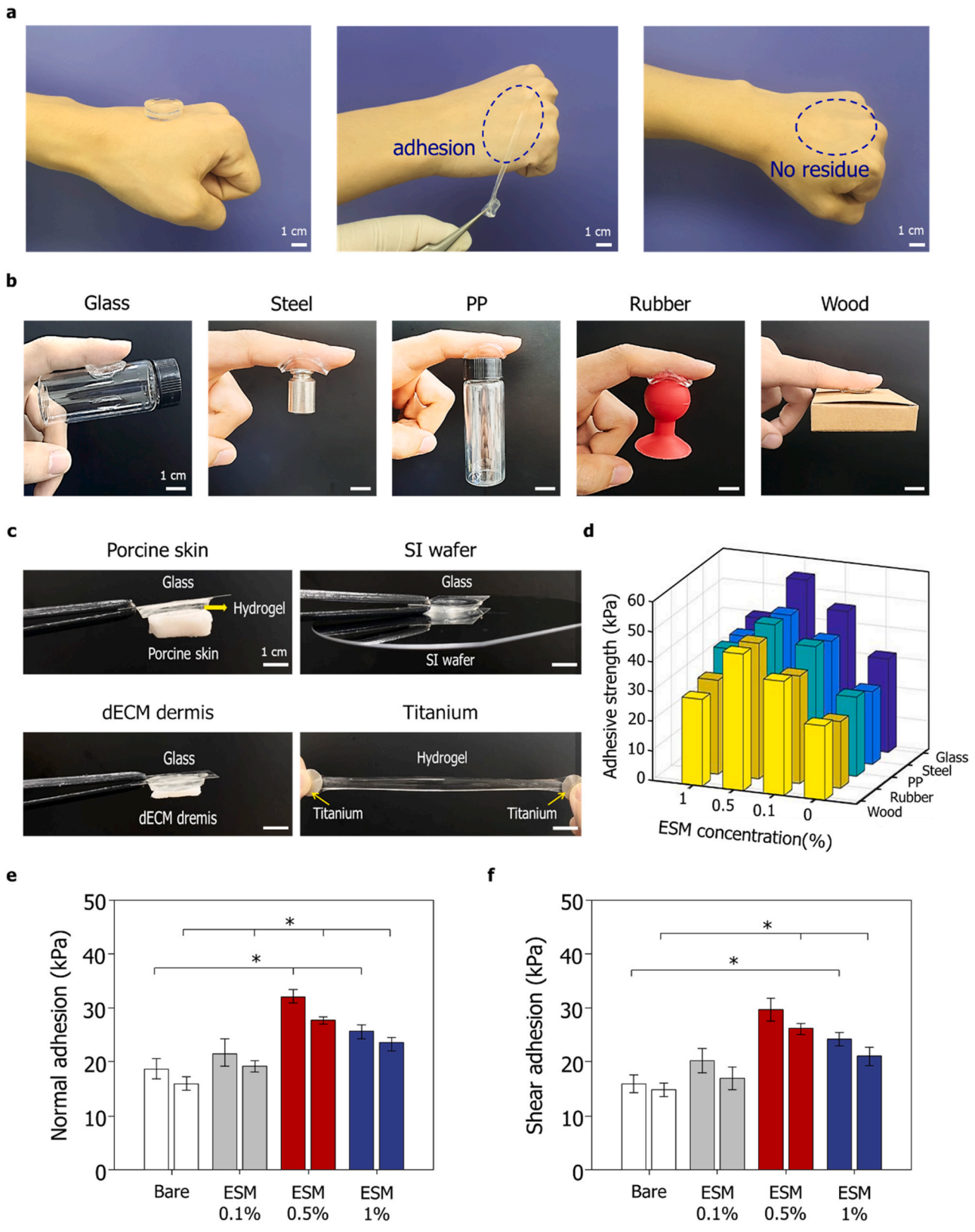

Fig. 2. Adhesive properties of ESM-incorporated hydrogels. (a) The fabricated hydrogel adhered well to the skin and left no residue or skin irritation after being peeled off. (b, c) The fabricated hydrogel (ESM 0.5 %) showed excellent adhesion to various surfaces: glass, steel, PP, rubber, wood, porcine skin, dECM dermis, SI wafer, and titanium. (d) Adhesive strength of the fabricated hydrogels (ESM 0 %, 0.1 %, 0.5 %, and 1 %) to various surfaces: glass, steel, PP, rubber, and wood. (e, f) Normal and shear adhesiveness of fabricated hydrogels (ESM 0 %, 0.1 %, 0.5 %, and 1 %) to porcine skin (left) and dECM dermis (right). PP, polypropylene; dECM, decellularized extracellular matrix; SI, silicon; ESM, eggshell membrane.

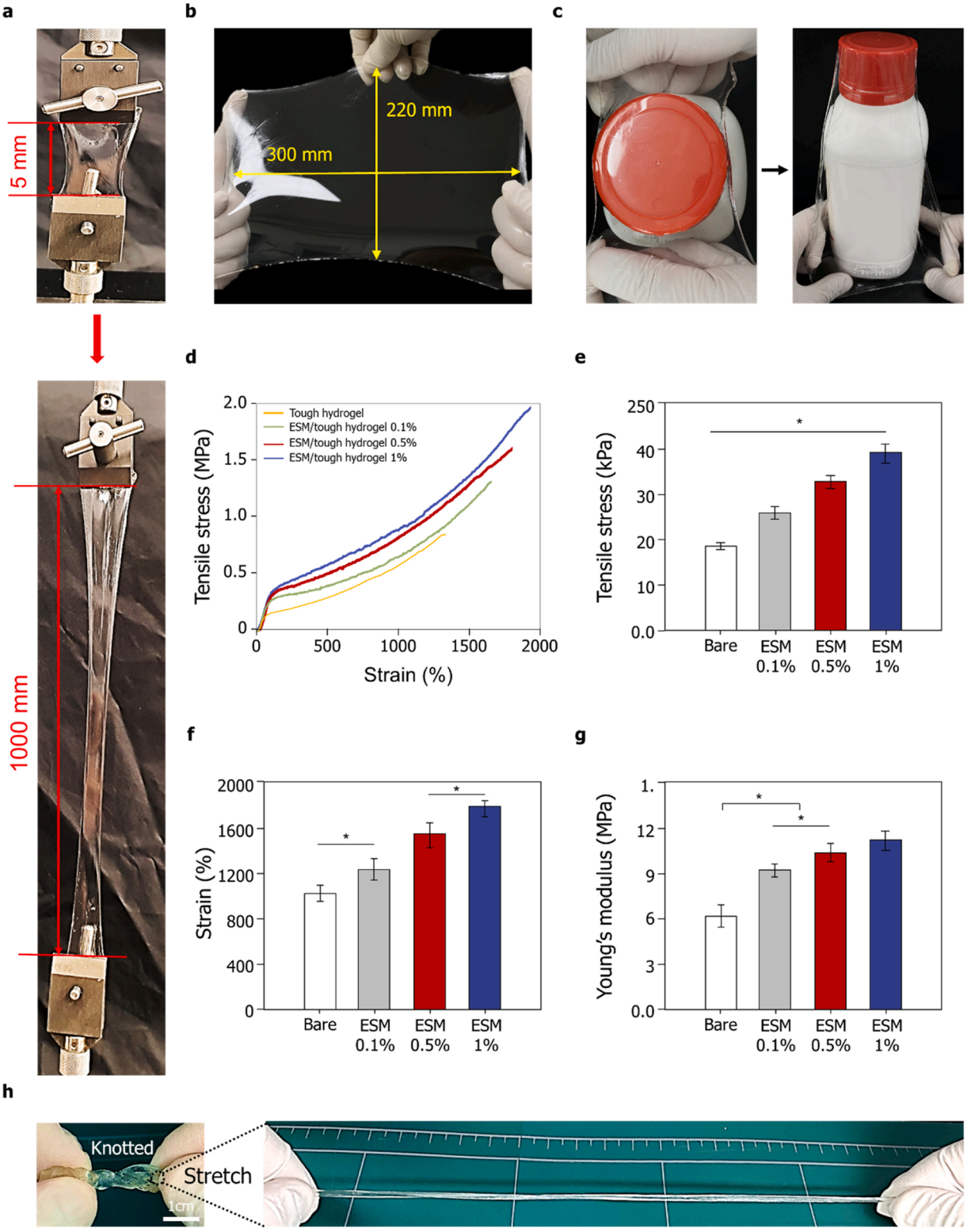

Fig. 3. Mechanical properties of ESM-incorporated hydrogels. (a) The fabricated hydrogel was elongated to 20 times its initial length. No residue or irritation on the skin was found after the hydrogel had been peeled off. (b) Square ESM-incorporated hydrogel showing 1600 % of areal expansion under biaxial tension. (c) Cylinder covered with the hydrogel membrane. (d) Strain–stress curves generated from tensile tests of hydrogels fabricated with various concentrations of ESM. (e–g) Tensile stress, strain, and Young's modulus of hydrogels fabricated with various concentrations of ESM. (h) Fabricated hydrogel that had been knotted and stretched up to 12 times its initial length. ESM, eggshell membrane.

of the increase in cross-linking by the higher amount of ESM particles present. Fig. 3e–g show the tensile stress, strain, and Young's (elastic) modulus of the hydrogels according to their ESM concentration. Specifically, the maximum tensile stress of the 1 % ESM-containing hydrogel was higher (38 kPa) than that of the control (bare) group (17 kPa). Additionally, its maximum strain (1850 %) and Young's modulus value (11.5 MPa) were also higher than those of the control group (950 % and 6 MPa, respectively). Even hydrogels that had been cut off and re-knotted could be stretched to more than 12 times their original length without fractures (Fig. 3h). The highly stretchability and toughness of the fabricated hydrogel were attributed to two factors. First, the strong bonds formed through the covalent cross-linking of the ESM particles with the polyacrylamide and alginate chains strengthen the hydrogel network. Indeed, the investigation of the fabricated hydrogels with different ESM concentrations (volume ratios of ESM to ESM + acrylamide) confirmed that the mechanical properties of the hydrogels were significantly improved with higher ESM concentrations. Second, the high density of hydrophilic functional groups in the ESM

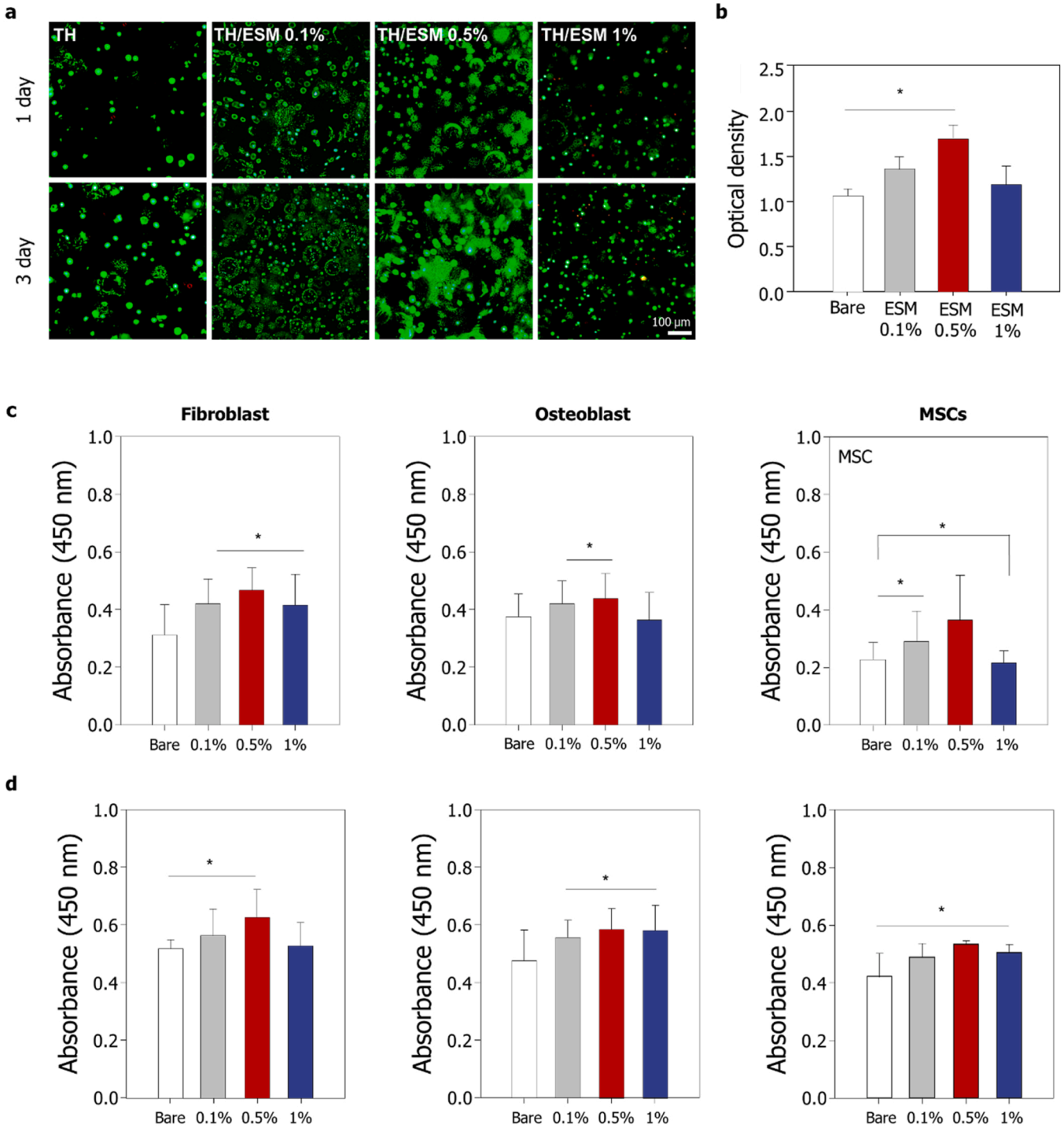

Fig. 4. Biocompatibility of various ESM-incorporated hydrogels. (a) Immunofluorescence microscopy images of fibroblasts on different hydrogels. (b) Optical density quantification of the number of fibroblasts on the hydrogels. (c, d) Optical density quantification of the number of fibroblasts, osteoblasts, and MSCs attached to various hydrogels for 1 h (c) and 3 day (d). ESM, eggshell membrane; TH, tough hydrogel; MSCs, mesenchymal stem cells.

allows the particles to be well dispersed within the hydrogel. Thus, the mechanical properties of the hydrogel were improved because of the reinforcement effects of the ESM particles.

3.4. Bioactive effects of the ESM-incorporated hydrogels

Cells demonstrated good affinity with the ESM-incorporated hydrogels, with improved adhesion and proliferation on the fabricated product. Immunofluorescence microscopy of NIH-3T3 fibroblasts cultured on the fabricated hydrogels showed them adhering well to the scaffold surface compared with the cells on an alginate–polyacrylamide-based hydrogel without ESM (used as a control for comparison). After 3 days of culture, a large number of fibroblasts had adhered to and proliferated well on the ESM-incorporated hydrogel, forming cell colonies (Fig. 4a). By contrast, fibroblasts were barely spread on the control hydrogel and were slow to proliferate. The number of cell colonies was higher on all ESM-incorporated hydrogels (especially in the 0.5 % ESM group) than on the control hydrogel, as determined by optical density quantification (Fig. 4b). To optimize the cell performance of the ESM-incorporated hydrogel, the adhesion and proliferation of fibroblasts, osteoblasts, and mesenchymal stem cells on constructs containing different ESM concentrations (0.1 %, 0.5 %, and 1 %) were investigated for 1 day and 3 day. Interestingly, all three types of cells showed higher adhesion and proliferation on the ESM-incorporated hydrogels than on the control hydrogel. Importantly, the 0.5 % ESM group showed the highest cell adhesion and proliferation for all three types of cells. These results indicate that the ESM plays a critical role in promoting cellular adhesion and proliferation on the hydrogels. Although the cytotoxicity of hydrogels has recently been reduced through the incorporation of natural polymers, such as alginate, the previously reported polyacrylamide-based tough hydrogels were still unsuitable for cell adhesion and proliferation. By contrast, the cell-friendly ESM-incorporated hydrogel fabricated in this study overcomes the issue of biocompatibility, which is a significant step forward for the tissue engineering application of tough hydrogels.

In summary, this study presents a simple method for the synthesis of tough, cell-friendly, highly stretchable, and ultra-adhesive hydrogels using ESMs. The fabricated hydrogel was strengthened through the covalent cross-links between the ESM particles and polyacrylamide and alginate chains. Moreover, the abundant amine and carboxyl functional groups of the ESM gave the hydrogel ultra-adhesive properties. Compared with the original alginate–polyacrylamide-based tough hydrogel, this current fabrication has the following advantages for tissue engineering applications: First, as the reinforcing agent of the hydrogel networks, the ESM contributes extreme stretchability and toughness to the fabricated scaffold. Second, as the donor of functional groups, the ESM enhances the tissue adhesiveness of the hydrogel. Third, as the bioactive agent, the ESM improves the cell affinity and biocompatibility of the hydrogel. In conclusion, the design principles of this study suggest a route for developing ultra-adhesive and tough hydrogels. The strategy of reinforcement with ESMs was used to overcome the limitations of previous hydrogels, which were not adhesive and were toxic to cells and tissue. This novel construct represents an important step forward in the design of a tough hydrogel that integrates cell-friendly and ultra-adhesive properties for tissue engineering purposes.

CRediT authorship contribution statement

Jangho Kim: Conceptualization, Methodology, Final approval. **Yonghyun Gwon:** Data analyzing, Methodology, Writing – original draft. **Sunho Park:** Methodology, Data analyzing. **Woochan Kim, Hyoseong Kim:** Writing – review & editing.

Declaration of Competing Interest

The authors declare the following financial interests/personal relationships which may be considered as potential competing interests: Jangho Kim reports financial support was provided by National Research Foundation. Jangho KIM reports a relationship with National Research Foundation of Korea that includes: funding grants.

Data Availability

Data will be made available on request.

Acknowledgements

This work was supported by National Research Foundation (NRF) grants funded by the Korea Government (NRF-2019R1I1A3A0106345, 2019M3A9H1103737, 2020R1A5A8018367, 2021M3E5E703044011, and 2022M3A9E4017151). The authors are grateful to the Center for Research Facilities at Chonnam National University for the assistance provided during the organic structure analyses (FE-SEM, XPS, and FTIR).

Appendix A. Supporting information

Supplementary data associated with this article can be found in the online version at doi:10.1016/j.colsurfb.2023.113156.

References

[1] J.-Y. Sun, X. Zhao, W.R. Illeperuma, O. Chaudhuri, K.H. Oh, D.J. Mooney, J. J. Vlassak, Z. Suo, Highly stretchable and tough hydrogels, Nature 489 (7414) (2012) 133–136.
[2] L. Han, X. Lu, K. Liu, K. Wang, L. Fang, L.-T. Weng, H. Zhang, Y. Tang, F. Ren, C. Zhao, Mussel-inspired adhesive and tough hydrogel based on nanoclay confined dopamine polymerization, ACS Nano 11 (3) (2017) 2561–2574.
[3] D. Gan, Z. Wang, C. Xie, X. Wang, W. Xing, X. Ge, H. Yuan, K. Wang, H. Tan, X. Lu, Mussel-inspired tough hydrogel with in situ nanohydroxyapatite mineralization for osteochondral defect repair, Adv. Healthc. Mater. 8 (22) (2019) 1901103.
[4] C.W. Peak, J.J. Wilker, G. Schmidt, A review on tough and sticky hydrogels, Colloid Polym. Sci. 291 (9) (2013) 2031–2047.
[5] D. Gan, W. Xing, L. Jiang, J. Fang, C. Zhao, F. Ren, L. Fang, K. Wang, X. Lu, Plant-inspired adhesive and tough hydrogel based on Ag-lignin nanoparticles-triggered dynamic redox catechol chemistry, Nat. Commun. 10 (1) (2019) 1–10.
[6] W. Chen, N. Li, Y. Ma, M.L. Minus, K. Benson, X. Lu, X. Wang, X. Ling, H. Zhu, Superstrong and tough hydrogel through physical cross-linking and molecular alignment, Biomacromolecules 20 (12) (2019) 4476–4484.
[7] M.C. Darnell, J.-Y. Sun, M. Mehta, C. Johnson, P.R. Arany, Z. Suo, D.J. Mooney, Performance and biocompatibility of extremely tough alginate/polyacrylamide hydrogels, Biomaterials 34 (33) (2013) 8042–8048.
[8] S. Park, K.S. Choi, D. Lee, D. Kim, K.T. Lim, K.-H. Lee, H. Seonwoo, J. Kim, Eggshell membrane: review and impact on engineering, Biosyst. Eng. 151 (2016) 446–463.
[9] A. Mittal, M. Teotia, R. Soni, J. Mittal, Applications of egg shell and egg shell membrane as adsorbents: a review, J. Mol. Liq. 223 (2016) 376–387.
[10] M. Baláž, Eggshell membrane biomaterial as a platform for applications in materials science, Acta Biomater. 10 (9) (2014) 3827–3843.
[11] M.K. Sah, S.N. Rath, Soluble eggshell membrane: a natural protein to improve the properties of biomaterials used for tissue engineering applications, Mater. Sci. Eng.: C 67 (2016) 807–821.
[12] S. Park, Y. Gwon, W. Kim, J. Kim, Rebirth of the eggshell membrane as a bioactive nanoscaffold for tissue engineering, ACS Biomater. Sci. Eng., 2021.
[13] R.A. Mensah, S.B. Jo, H. Kim, S.-M. Park, K.D. Patel, K.J. Cho, M.T. Cook, S. B. Kirton, V. Hutter, L.E. Sidney, The eggshell membrane: a potential biomaterial for corneal wound healing, J. Biomater. Appl. (2021), 08853282211024040.
[14] D. Kim, Y. Gwon, S. Park, W. Kim, K. Yun, J. Kim, Eggshell membrane as a bioactive agent in polymeric nanotopographic scaffolds for enhanced bone regeneration, Biotechnol. Bioeng. 118 (5) (2021) 1862–1875.
[15] S. Park, T. Kim, Y. Gwon, S. Kim, D. Kim, H.-H. Park, K.-T. Lim, H.E. Jeong, K. Kim, J. Kim, Graphene-layered eggshell membrane as a flexible and functional scaffold for enhanced proliferation and differentiation of stem cells, ACS Appl. Bio Mater. 2 (10) (2019) 4242–4248.
[16] H. Jung, M.K. Kim, J.Y. Lee, S.W. Choi, J. Kim, Adhesive hydrogel patch with enhanced strength and adhesiveness to skin for transdermal drug delivery, Adv. Funct. Mater. 30 (42) (2020) 2004407.
[17] C. Wang, C.-K.D. Ma, H. Yeon, X. Wang, S.H. Gellman, N.L. Abbott, Nonadditive interactions mediated by water at chemically heterogeneous surfaces: nonionic polar groups and hydrophobic interactions, J. Am. Chem. Soc. 139 (51) (2017) 18536–18544.
[18] Y. Yang, P. Qi, Y. Ding, M.F. Maitz, Z. Yang, Q. Tu, K. Xiong, Y. Leng, N. Huang, A biocompatible and functional adhesive amine-rich coating based on dopamine polymerization, J. Mater. Chem. B 3 (1) (2015) 72–81.

[19] D. Yang, X. Wan, P. Quan, C. Liu, L. Fang, The role of carboxyl group of pressure sensitive adhesive in controlled release of propranolol in transdermal patch: quantitative determination of ionic interaction and molecular mechanism characterization, Eur. J. Pharmaceut. Sci. 115 (2018) 330–338.
[20] Y. Wang, C. Xie, P. Wang, X. Wang, C. Wang, X. Xun, H. Teng, An elastic gel consisting of natural polyphenol and pluronic for simultaneous dura sealing and treatment of spinal cord injury, J. Control. Release 323 (2020) 613–623.
[21] Z. Zhang, C. He, Y. Rong, H. Ren, T. Wang, Z. Zou, X. Chen, A fast and versatile cross-linking strategy via o-phthalaldehyde condensation for mechanically strengthened and functional hydrogels, Natl. Sci. Rev. 8 (4) (2021), nwaa128.
[22] K. Liu, H. Yang, G. Huang, A. Shi, Q. Lu, S. Wang, Y. Lv, Adhesive anastomosis for organ transplantation, Bioact. Mater. 13 (2022) 260–268.